Thermochimica Acta, 191 (1991) 63–94
Elsevier Science Publishers B.V., Amsterdam

Preparation of Pd/SiO_2 catalysts for methanol synthesis Part II. Thermal decomposition of $[Pd(NH_3)_4]^{2+}/SiO_2$

Adrián L. Bonivardi [1] and Miguel A. Baltanás [2]

INTEC [3], Güemes 3450, 3000-Santa Fe (Argentina)

(Received 20 March 1991)

Abstract

As a part of an experimental program aimed at the systematic analysis of the controlled deposition of Pd/SiO_2 on well characterized macroporous and microporous silica gels (Davison G-59, 254 $m^2\ g^{-1}$ and G-03, 558 $m^2\ g^{-1}$) the nature of the surface species upon drying and thermal decomposition of the tetramminepalladium complex (TPSiO) obtained by ion exchange (IE) of palladium acetate in aqueous ammonium hydroxide (Pd loading: 0.5–11%Pd w/w), has been systematically followed by the combined use of diffuse reflectance spectroscopy (DRS), differential scanning calorimetry (DSC), thermogravimetric analysis (TG), X-ray diffraction (XRD) and X-ray photoelectron spectroscopy (XPS).

DRS indicates that drying in air ($T \approx 393$ K) leaves a stable diamminepalladium complex (DPSiO) on the surfaces.

Decomposition of DPSiO upon calcination in inert and oxidizing atmospheres was studied from 308 to 773 K, with heating rates of 4–64 K min^{-1} (N_2) and 2–32 K min^{-1} (air).

Two decomposition zones are identified with DSC and TG. (1) In the low-temperature region (308–473 K) endothermal signals which correspond to a liberation of NH_3 around 359 K (G-59) or 371 K (G-03) were observed; (2) the high-temperature region (473–773 K) only shows endothermal peaks when N_2 is used, but in air several signals indicate that a sequence of transformations of the Pd occurs.

Ultradispersed Pd^0 is the final product on both catalyst types when N_2 is the decomposing atmosphere, whereas either a mixture of $Pd^0 + [(SiO)_2]^{2-}\,Pd^{2+}$ (on the microporous G-03) or pure $[(SiO)_2]^{2-}\,Pd^{2+}$ (on the macroporous G-59) are the final products when air is employed.

INTRODUCTION

The rational preparation of a supported metal catalyst calls for an in-depth knowledge, via systematic studies, of each of the variables that may

[1] Research Assistant from CONICET.

[2] Member of CONICET's Scientific and Technological Research Staff and Professor at U.N.L.

[3] Instituto de Desarrollo Tecnológico para la Industria Química. Universidad Nacional del Litoral (U.N.L.) and Consejo Nacional de Investigaciones Científicas y Técnicas (CONICET).

play a role during such preparation process. This process starts with the impregnation/sorption of a certain precursor, usually a salt or complex of the metal cation, through incipient wetness or ion exchange methods, and ends with a final reduction stage aimed at obtaining metal crystallites of the desired size, stability and/or dispersion. The procedure, though, normally includes intermediate operations such as washing, drying and calcination whose process conditions are relevant for the attainment of a given catalytic performance [1,2].

Despite these observations, relatively few works have as yet been published regarding to the systematic analysis of the preparation steps of Pd/SiO_2, a widely used catalytic material. In a previous paper [3] we reported that it is possible to use ion exchange (IE) methods to obtain precursors of Pd metal catalysts, supported on commercial gels of silica having widely different structures, in a controlled fashion. Halide free amminepalladium complexes prepared from palladium acetate in aqueous alkaline solutions were employed, with Pd loadings in the 0.5–11% w/w range. The ion exchange and washing stages were followed in detail, and it was shown that the $[Pd(NH_3)_4]^{2+}$ complex adsorbs on these gels of silica at pH 11 without any exchange of NH_3 ligands, but that NH_3 and H_2O are exchanged whenever washings are made with distilled deionized water (pH 6.5).

This work reports on the influence of the drying and thermal decomposition conditions on these ion exchanged, washed systems. Drying operating conditions, calcination under inert and oxidizing atmospheres as well as thermal histories of catalytic precursors onto these solids are thoroughly examined.

Drying conditions of adsorbed metal complexes have usually been ignored in the interpretation of experimental results. However, Gubitosa et al. [4] postulated that the IE of $[Pd(NH_3)_4]^{2+}$ on silica, after drying their samples at 393 K, gives *cis*-$(-SiO)_2Pd(NH_3)_2$ on the support surface. A similar structure of the surface complex had been proposed for the IE of Cu^{2+} in basic media [5,6], but Amara et al. [7] reported instead the presence of the $[Cu(NH_3)_2(H_2O)_2]^{2+}$ surface complex after drying $[Cu(NH_3)_4]^{2+}$ ion exchanged samples at 353 K.

Likewise, scant attention has been paid to the thermal decomposition conditions of the supported metal catalyst precursors, with the notable exception of zeolitic systems. Thus, Spector et al. [8] observed the formation of metal particles of poor dispersion and a broad size distribution in an HY faujasite exchanged with Pd^{2+}, during the thermal treatment in vacuo of a sample which had been previously exposed to water vapor, whereas the decomposition of $[Pt(NH_3)_4]^{2+}$ ion exchanged on a Y zeolite gave rise to products with very different metal dispersions when the complex was exposed to either oxidizing or reducing conditions while its decomposition was made [9].

Reagan et al. [10] have correlated the results of the thermal decomposition under different atmospheres of amminepalladium complexes ion exchanged on Y zeolites with the final dispersion of the metal crystallites and the catalytic properties of these materials. They have shown that when the departing metal complex is $[Pd(NH_3)_4]^{2+}$ thermal decomposition under air leads (mostly) to surface Pd^{2+}, but that under helium or nitrogen streams Pd^0 are obtained instead. Homeyer and Sachtler [11,12], by contrast, paid closer attention to the relationship between the calcination temperature in air and the final size of the Pd crystallites, also using $[Pd(NH_3)_4]^{2+}$ ion exchanged on NaY. They found that the highest dispersions were attained whenever Pd^{2+} ions were kept in the zeolite supercavities and the diammine to tetrammine ratio was maximized during the calcination process.

Summarizing, the marked influence of the thermal decomposition and/or calcination conditions on the reproducibility of the final dispersion of the metal crystallites on zeolitic supports is by now widely acknowledged. It is then to be hoped that the same degree of knowledge is of value in the case of other supported systems, such as the Pd/SiO_2 catalysts hereby examined.

EXPERIMENTAL

Materials

Catalyst samples were obtained via IE of $[Pd(NH_3)_4]^{2+}$, prepared from 99.5% w/w palladium acetate purchased from Engelhard, on two commercial gels of silica (Davison, G-59 and G-03) in aqueous alkaline solution, at pH 11 and 298 K, with a maximum Pd loading of 11% w/w.

The supports were previously crushed and sieved through an 80-mesh Tyler screen, purified, calcined at 773 K, and then characterized by XRD, IR, sorptometry and porosimetry. G-59 is a macroporous solid whereas G-03 presents a microporous structure: Their BET (N_2) surface areas are 254 and 558 $m^2\ g^{-1}$, and their characteristic modal radii are 83 and 16 Å, respectively.

A detailed description of the methodology and experimental conditions used for the IE is given elsewhere [3].

Gas chromatography grade air and UHP nitrogen (99.9995%, Scott) were used.

Drying

Diffuse reflectance spectroscopy (DRS) was employed for the identification of the resulting amminepalladium complexes on the catalyst surfaces after the completion of several different drying procedures. Palladium loadings of about 2%Pd w/w (2.50 and 2.02%Pd w/w on G-59 and G-03, respectively) were found to be satisfactory to yield good signals. Samples

were coded indicating Pd nominal loading, support type and pH of washing (either 6.5 or 11 [3]). Thus, for instance, 2G-03/11 indicates a catalyst sample with 2%Pd w/w loading on G-03, washed at pH 11.

Pellets of 2.5 cm diameter and 0.3 cm thickness were obtained by pressing the wet cakes of the ion exchanged, washed solids at 20 kg cm^{-2}. Spectra were taken after each of the drying treatments at room temperature (RT), exposing the pellets to atmospheric conditions, with a UV-VIS-NIR Varian (Cary 17-D) spectrometer furnished with an integrating sphere covered with barium sulfate. Blank spectra from G-59 and G-03 were also taken to properly normalize data.

The samples of the 2G-59 catalyst were dried as follows: (A) in air (313 K) during 24, 48 and 72 h, or (B) under vacuum (20 kPa, 313 K). After either of these procedures was completed, a subsequent drying treatment, (C), was made with each of the pellets previously subjected to the first dryings by heating them under a stream of air from 313 to 393 K (200 ml min^{-1} (at STP) and 4 K min^{-1}) and then holding the upper temperature for 2 h.

Catalyst 2G-03 underwent only the (B) and (C) drying treatments, but procedure (C) was repeated a second time on these pellets.

The (A) type drying was performed in a forced convection stove; type (B) in a vacuum oven and type (C) in a horizontal oven attached to a linear temperature programmer, using an all-glass device. A maximum temperature difference of ± 0.2 K between the pellet center and its rim was measured when the cross flow of air was 200 ml min^{-1} (at STP). Cylinder air was used, without further purification, in all these drying experiments.

Thermal decomposition

The decomposition of the ion exchanged amminepalladium complexes was studied by means of differential scanning calorimetry (DSC), thermogravimetric analysis (TG) and X-ray diffraction (XRD) at atmospheric pressure. X-Ray photoelectron spectroscopy (XPS) was also employed for further characterization. Catalyst samples loaded with 3.57–10.27%Pd w/w, washed at pH 11 and then vacuum dried during 24 h (20 kPa, 313 K), were used for these studies. All the samples contained submonolayer coverages of Pd. Their characteristics and coding are indicated in Table 1.

DSC measurements were made in a Mettler DSC-30 unit, decomposing the Pd/SiO_2 precursors in the 308–773 K range. Temperature and heat flow readings were calibrated with nitrogen and air, using standard crucibles containing precise amounts of In, Pb and Zn. Their melting points (429.7, 600.5 and 692.6 K, respectively) were used for the calibration of temperature. The heat of fusion of In (28.45 J g^{-1}) was employed to set accurate values of the heat flow.

TABLE 1

Characteristics and coding of the catalyst samples used in the differential scanning calorimetry (DSC) and thermogravimetric (TG) experiments [a]

Silica support [b]	Palladium loading (%Pd w/w)	Pd surface coverage ($\theta = \Gamma_i/\Gamma_s$) [c]	Catalyst code sample
G-59	3.57	0.60	3G-59
	5.03	0.85	5G-59
G-03	3.98	0.37	4G-03
	7.48	0.70	7G-03
	10.27	0.96	10G-03

[a] After ion exchange (IE) of TPAcO in aqueous alkaline solution ($R = 30 \pm 0.5$ ml solution per g support, pH 11 and $T = 297$ K), and then washing at pH 11.

[b] Davison Types (W.R. Grace & Co.).

[c] Γ_i, initial value; Γ_s, saturation value; in units of mmol Pd m^{-2} [3].

Physical admixtures of $Pd(NH_3)_4Cl_2 \cdot H_2O$ with G-59 (5.6%Pd w/w, coded MG-59) and with G-03 (7.1%Pd w/w, coded MG-03) were decomposed in nitrogen (150 ml min^{-1} (at STP) and 8 K min^{-1}) to verify the absence of heat transfer artifacts, taking as the reference the enthalpy of (endo)thermal decomposition of *trans*-$(NH_3)_2PdCl_2$ [13] between 353 and 546 K. The total enthalpy changes for the decomposition of the MG-59 and MG-03 admixtures were 509 and 489 kJ (mol Pd)$^{-1}$ respectively (122 and 117 kcal (mol Pd)$^{-1}$). Since these values were the expected ones, and their difference was only 5%, heat transfer-related artifacts or difficulties were ruled out.

Catalyst samples were placed in aluminum crucibles (0.58 mm internal diameter; 40 μl volume) using as a reference an identical, empty unit. Approximate bed heights for the *i*G-59 and *i*G-03 samples were 1.1 mm and 0.4 mm respectively.

Three types of DSC studies were made under both oxidizing and inert atmospheres in each case. In the first one, the heating rate (β) was varied from 2 to 32 K min^{-1} in air (150 ml min^{-1} (at STP)) and from 4 to 64 K min^{-1} in N_2 (150 ml min^{-1} (at STP)), loading approximately similar amounts of Pd on the crucibles and catalysts of similar surface coverages (θ) from both supports. Thus, 4.7 mg of the 5G-59 catalyst ($\theta = 0.70$) and 5.2 mg of the 7G-03 ($\theta = 0.85$) were used in these runs. In the second study, the amount of Pd that was put into the crucibles was changed while keeping a constant total catalyst mass, by varying the Pd loading and/or surface coverage. Runs were made using 10.6 mg of *i*G-59 and 7.8 mg of *i*G-03, with a flow rate of N_2 or air of 150 ml min^{-1} (at STP) and $\beta = 8$ K min^{-1}. Finally, the gas flow rate (N_2 or air) was changed over selected catalyst samples: 5G-59 and 7G-03, with $\beta = 8$ K min^{-1}.

Two sets of the purified, calcined G-59 and G-03 support powders were also used as blank control samples: (i) air dried at 393 K for 2 h, and (ii)

soaked and washed with diluted NH_4OH(aq.) at pH = 11, then vacuum dried during 24 h (20 kPa, 313 K). This second procedure mimicked the one used with the catalysts.

For the DSC experiments the air was purified with a trap of 5 Å molecular sieve (Fisher Co.) followed by a second trap containing granulated ascarite (Riedel de Haën, pro-analysis). Nitrogen was only purified with a 5 Å molecular sieve.

The results from DSC were used to perform non-isothermal kinetic analyses.

X-Ray diffraction was employed as a control using a Rich Seifert JSO-Debyeflex Model 2002 unit with a Cu source and Ni filters.

Finally, thermogravimetric experiments were made using samples of 5G-59 and 7G-03 together with blanks of both supports dried at 393 K (2 h), using a Cahn Model RG electrobalance with a linear temperature program of $\beta = 6$ K min^{-1} and a gas flow rate (N_2 or air) of 15 ml min^{-1} (at STP). Both gases were prepurified with 5 Å molecular sieve; MnO/celite trap was also added, upstream the 5 Å cartridge, in the N_2 line.

Complementary XPS spectra of the thermally decomposed palladium complexes on selected catalyst samples (5G-59 and 7G-03), previously air dried at 313 K, were taken in a Shimadzu 750 ESCA spectrometer using monochromatic Mg Kα radiation ($h\nu = 1253.6$ eV). The normal operating vacuum pressure was less than 4×10^{-8} Torr. Binding energies (BE) were referenced to the Si 2p peak position of the supports, which was assigned a value of 103.2 eV [14]. Binding energy values are accurate to within ± 0.2 eV.

The catalyst samples were treated in a Pyrex tube reactor. A gas flow rate (N_2 or air) of 150 ml min^{-1} (at STP) and $\beta = 8$ K min^{-1} were employed while heating from 298 to 673 K in either inert or oxidizing atmospheres. In addition, a direct reduction at 473 (2 h) of an aliquot of 7G-03 with 150 ml min^{-1} (at STP) ($\beta = 2$ K min^{-1}) of ultra high pure hydrogen (Scott UHP 99.999%), was included for reference purposes. Hydrogen was prepurified with 5 Å molecular sieve and MnO/celite cartridges. After the completion of each of the decomposing or reducing treatments the catalyst samples were cooled under the same (reducing, inert or oxidizing) atmosphere in the tube reactor, then transferred and stored in a desiccator prior to their subsequent use for the XPS study.

RESULTS

Drying

Figures 1–3 show the DRS spectra of the catalyst samples dried under the above-mentioned conditions. The location of the absorption bands of amminepalladium complexes in aqueous solution is also included in these

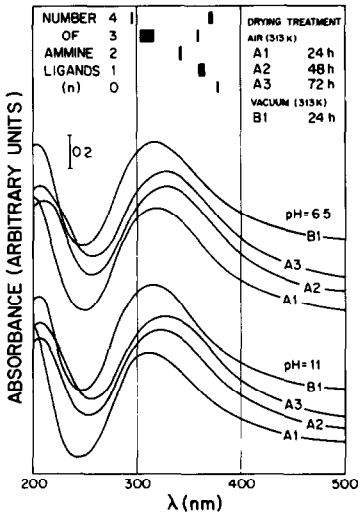

Fig. 1. DRS spectra of aquoamminepalladium complexes adsorbed onto G-59 (ion exchanging with TPAcO at pH 11, then washing at pH 11 and 6.5) after the following drying treatments: Type A (in air, at 313 K) and Type B (in vacuum oven, 20 kPa, at 313 K). The upper part of the figure shows the location of the absorption bands of $[Pd(NH_3)_n(H_2O)_{4-n}]^{2+}$ in aqueous solution [3].

figures. Each of the drying procedures led to bathochromic shifts of the absorption maxima (Table 2), from the initial location of the ion exchanged $[Pd(NH_3)_4]^{2+}$ complex adsorbed on the wet catalysts (298 nm and shoulder at 370 nm). This is obviously linked to the loss of NH_3 ligands, since the absorption maxima of $[Pd(NH_3)_n(H_2O)_{4-n}]^{2+}$ complexes progressively shift from 300 to 370 nm when n decreases from 4 to 0.

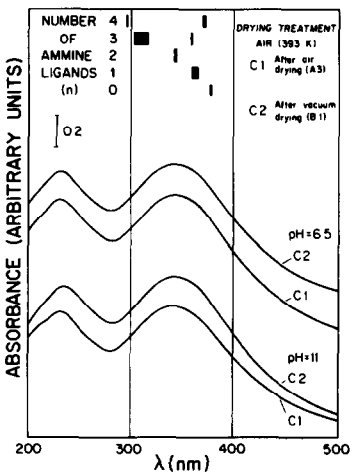

Fig. 2. DRS spectra of aquoamminepalladium complexes adsorbed onto G-59 (ion exchanging with TPAcO at pH 11, then washing at pH 11 and 6.5) after drying treatment Type C (in a stream of air 200 ml min^{-1} (at STP), at 393 K, for 2 h).

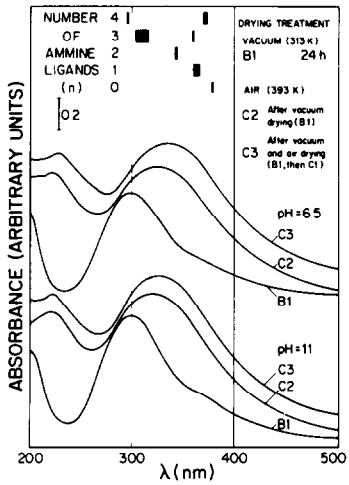

Fig. 3. DRS spectra of aquoamminepalladium complexes adsorbed onto G-03 (ion exchanging with TPAcO at pH 11, then washing at pH 11 and 6.5) after different drying treatments. Operating conditions are the same as in Figs. 1 and 2.

When pellets of 2G-59 washed at pH 11 and 6.5 (2G-59/11 and 2G-59/6.5) were dried in air at 313 K, the (A) type air drying procedure, their absorption maxima shifted to about the same location after 24 h. The shift was slightly more pronounced in the samples washed at pH 6.5 which indicated that both solids had lost equivalent amounts of NH_3 ligands after this drying period. Further exposure to drying (48 then 72 h) led to about

TABLE 2

DRS maxima of the UV-VIS absorption bands of the adsorbed aquoamminepalladium complexes on G-59 and G-03 silica gels after ion exchange (IE) and drying treatments

Sample code [a]	Absorption maximum, λ (nm)							
	Wet pellet	After drying treatments						
		Type A (air, 313 K)			Type B (vacuum, 313 K)	Type C [b] (air, 393 K)		
		A1 (24 h)	A2 (48 h)	A3 (72 h)	B1 (24 h)	C1 (A3 [c])	C2 (B1 [c])	C3 (B1 + C2 [c])
2G-59/11	300	310	323	326	315	343	346	
2G-59/6.5	301	320	327	327	317	348	348	
2G-03/11	298, 370(sh)				300		323	330
2G-03/6.5	298, 370(sh)				300		325	335

[a] Code indicates: Pd nominal loading, support type and pH of washing.

[b] With air flow 200 ml min^{-1} (at STP), from 313 to 393 K at 4 K min^{-1}, then holding for 2 h at the upper temperature.

[c] Previous drying regime.

the same ligand losses. The (B) type vacuum drying gave similar results to the ones obtained from the (A) type drying after 24 h (Table 2). The (C) type drying treatment, i.e. a crossflow of drying air for 2 h at 393 K, on the 2G-59 pellets which had been previously dried under (A) or (B) conditions led to almost identical locations of their absorption maxima, around 346 nm.

No significant changes could be observed between the DRS spectra of wet and vacuum dried 2G-03 pellets, with the exception of a more pronounced signal of the 370 nm shoulder from the $[Pd(NH_3)_4]^{2+}$ species in the 2G-03/11 catalyst. Two subsequent consecutive dryings, each time for 2 h, at 393 K under a crossflow of air led to progressive losses of ligands, with absorption maxima displaced to 323–325 nm, then to 330–335 nm (Fig. 3 and Table 2).

In broad terms, then, the bathochromic shifts, as related to the location of the absorption maxima in the wet pellets, were larger for the 2G-59 than for the 2G-03 samples and also (marginally) larger for the catalyst powders washed at the lower pH.

Thermal decomposition

The set of DSC runs made apparent the existence of two well defined zones with different thermal evolutions: (a) a low temperature region (from 308 to about 473 K), and (b) a high temperature one (up to about 680 K). Following that finding, DSC and TG experiments are presented within this low-temperature/high-temperature framework.

Low-temperature region

Endothermal DSC signals evolved in the 308–473 K region, regardless of the kind of decomposition atmosphere that was used. Figure 4 shows the characteristic DSC spectra for the thermal decomposition of 5G-59 and 7G-03 in air (150 ml min^{-1} (at STP), $\beta = 8$ K min^{-1}), together with those of the untreated (i.e. simply dried) and treated (i.e. washed at pH 11 with aqueous NH_4OH) supports.

A single, broad endothermal peak with a minimum around 359 K was typical of the 5G-59 catalyst, whereas the 7G-03 showed two endothermal evolutions with minima around 319 and 371 K. These last two peaks merged into one whenever higher heating rates were tried. Thermal decomposition in nitrogen gave almost identical DSC evolutions in this region.

Blanks of the pure G-59 and G-03 silicas, whether treated with the alkaline solution or not, also gave endothermal DSC evolutions, their peaks being broader in the first case. The peak minima of the G-59 blank samples were located at lower temperatures than those of G-03 and also the peak minima of the untreated blanks were located at lower temperatures than their treated counterparts.

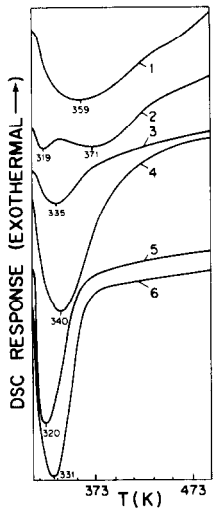

Fig. 4. Differential scanning calorimetry (DSC) spectra upon thermal decomposition in air (150 ml min^{-1} (at STP), $\beta = 8$ K min^{-1}) of adsorbed amminepalladium complexes on G-59 and G-03 silica gels, in the low-temperature region: (1) 5G-59; (2) 7G-03; (3) G-59 blank, treated at pH 11; (4) G-03 blank, treated at pH 11; (5) G-59 blank, untreated, air dried at 393 K; and (6) G-03 blank, untreated, air dried at 393 K.

Since these samples were transferred to the DSC apparatus prior to the thermal decomposition run itself while exposing them to the room atmosphere, the adsorption of a certain amount of water vapor onto the gels of silica was foreseen. Trial runs showed that although the peak areas were dependent upon the exposure time to the room atmosphere, the peak minima were not.

Recalling that the DRS experiments indicated the loss of NH_3 ligands from the supported $[Pd(NH_3)_4]^{2+}$ complex up to 393 K (type (C) drying) it follows from the DSC spectra (Fig. 4) that the 5G-59 catalyst loses water and ammonia jointly whereas 7G-03 sheds these compounds in a sequential fashion.

Thermogravimetric experiments confirmed this conclusion: blank samples of G-59 and G-03 which had been previously dried at 393 K for 2 h showed weight losses up to 423 K, under both N_2 or air "decomposition" atmospheres, with further constant weight. Likewise, TG analyses of the 5G-59 and 7G-03 catalysts indicated a steady, smooth weight loss extending until about 473 K, regardless of the type of decomposition atmosphere.

High temperature region

The decomposition of the amminepalladium complexes under inert atmosphere was characterized by the evolution of a single endothermal DSC peak in the 530–680 K temperature range. This behavior was reproducible provided that sufficiently high gas flow rates (larger than 20 ml min^{-1} (at STP))

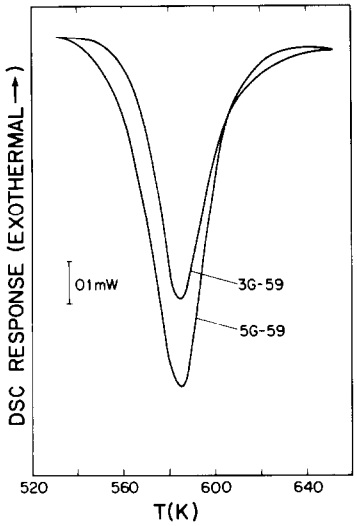

Fig. 5. DSC spectra of the energy evolutions upon thermal decomposition in nitrogen (150 ml min^{-1} (at STP), $\beta = 8$ K min^{-1}) of adsorbed amminepalladium complexes on G-59 silica gel versus palladium loading in the DSC crucible normalized to an identical sample mass of 10 mg (high temperature region).

were employed, to prevent deleterious signals arising from the incomplete air removal from the samples after purging the DSC chamber.

The thermal evolutions of the decomposing complexes under oxidizing conditions were exothermal instead, and the features of the DSC spectra were dependent upon the type of silica support. Several peaks were observable in the 450–680 K range; their amount, location and relative sizes changed whenever the heating rate or the air flow rate were varied.

Blanks with pure G-59 and G-03 had flat DSC spectra using either inert or oxidizing atmospheres in this high temperature region.

A more detailed examination of both situations follows now.

Inert atmosphere. Figures 5 and 6 show the DSC spectra of the *i*G-59 and *i*G-03 catalyst samples upon decomposition of different amounts of the adsorbed amminepalladium complexes with N_2 (150 ml min^{-1} (at STP), $\beta = 8$ K min^{-1}), as indicated in the Experimental section.

With both silicas a single endothermal peak evolved, around about the same temperature interval, its minimum being displaced somewhat towards lower temperatures the higher the palladium loading on the crucibles. Table 3 shows that the experimental enthalpy changes, ΔH_t^N (expressed as kJ (mol Pd)$^{-1}$) were independent of the amount of palladium loaded on the crucibles, for a nitrogen flow rate of 150 ml min^{-1} (at STP), but also that these enthalpy changes were substantially different for the macroporous and the microporous silica supports, the enthalpy change values being almost double on the latter (G-03).

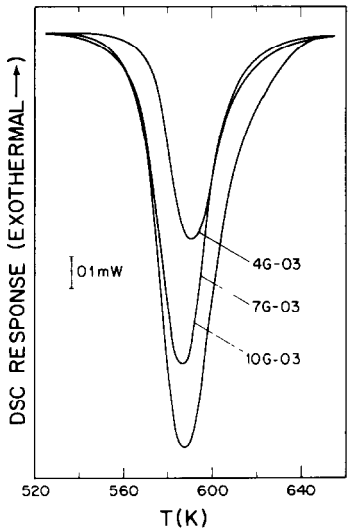

Fig. 6. DSC spectra of the energy evolutions upon thermal decomposition in nitrogen (150 ml min^{-1} (at STP), $\beta = 8$ K min^{-1}) of adsorbed amminepalladium complexes on G-03 silica gel versus palladium loading in the DSC crucible normalized to an identical sample mass of 10 mg (high temperature region).

TABLE 3

DSC energy evolutions and peak positions upon thermal decomposition in nitrogen of amminepalladium complexes ion exchanged on G-59 and G-03 silica gels relative to palladium loading in the DSC chamber and gas flow rate (high temperature region) [a]

Sample code	Nitrogen flow rate (ml min^{-1} (at STP))	Sample mass [b] (mg)	Pd loaded in the DSC chamber (mmol × 10^3)	Number of DSC peaks	Peak position (K)	Thermal evolution ΔH_t^N (kJ (mol Pd)$^{-1}$)
3G-59	150	10.13	3.28	1	585	36.7
5G-59	150	10.31	4.64	1	584	34.4
	80	9.12	4.10	1	582	30.0
	20	10.66	4.80			
4G-03	150	7.57	2.72	1	590	76.8
7G-03	150	8.25	5.40	1	587	72.7
	80	7.65	5.00	1	588	73.8
	20	7.71	5.04			
10G-03	150	7.72	6.76	1	587	76.5

[a] Heating rate, $\beta = 8$ K min^{-1}.
[b] Dry basis.

TABLE 4

DSC energy evolutions and peak positions upon thermal decomposition in nitrogen of amminepalladium complexes ion exchanged on G-59 and G-03 silica gels relative to heating rate (high temperature region) [a]

Sample code	Heating rate, β (K min^{-1})	Sample mass [b] (mg)	Pd loaded in the DSC chamber (mmol$\times 10^3$)	Number of DSC peaks	Peak position (K)	Thermal evolution ΔH_t^N (kJ (mol Pd)$^{-1}$)
5G-59	4	10.36	4.66	1	571	38.1
	8	10.31	4.64	1	584	34.4
	16	10.86	4.89	1	596	36.6
	32	10.85	4.88	1	602	36.9
	64	10.56	4.75	1	616	27.7
7G-03	4	7.90	5.17	1	579	77.9
	8	8.25	5.40	1	587	72.7
	16	7.82	5.11	1	597	76.2
	32	7.99	5.23	1	610	73.6
	64	7.88	5.15	1	619	63.4

[a] Nitrogen flow rate, 150 ml min^{-1} (at STP).
[b] Dry basis.

The same results were obtained when the nitrogen flow rate was reduced from 150 to 80 ml min^{-1} (at STP), but lower gas flow rates could not be employed without provoking spurious signals, as already stated.

When the heating rate (β) was varied from 4 to 64 K min^{-1} (N_2 flow rate, 150 ml min^{-1} (at STP)) the same spectral features were found using 5G-59 and 7G-03, provided $\beta \leqslant 32$ K min^{-1}. The enthalpy change values were again almost double on the microporous silica supported palladium catalyst. Table 4 also shows that the minima of the endothermal peak were located at about the same values for identical heating rates on both catalysts.

Oxidizing atmosphere. Figures 7 and 8 show the DSC spectra of the *i*G-59 and *i*G-03 catalyst samples upon decomposition of different amounts of the adsorbed amminepalladium complexes in air (150 ml min^{-1} (at STP), $\beta = 8$ K min^{-1}), as indicated in the Experimental section.

These DSC spectra were distinctive of each support. Firstly, the amminepalladium complex decomposed at lower temperature on *i*G-59 than on *i*G-03. Secondly, only two convoluted decomposition peaks appeared in the G-59 supported catalysts whereas three consecutive exothermal evolutions characterized the decomposition of the complex on the microporous G-03, the relative area of the third increasing with increasing amount of palladium placed in the crucible.

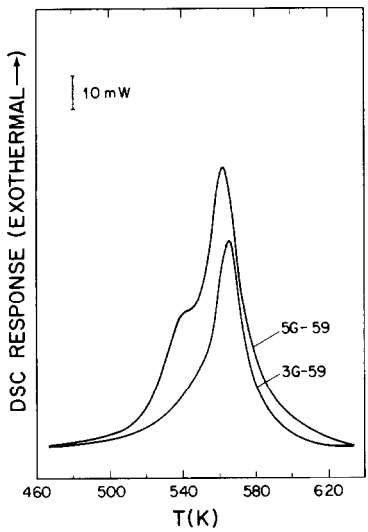

Fig. 7. DSC spectra of the energy evolutions upon thermal decomposition in air (150 ml min^{-1} (at STP), $\beta = 8$ K min^{-1}) of adsorbed amminepalladium complexes on G-59 silica gel versus palladium loading in the DSC crucible normalized to an identical sample mass of 10 mg (high temperature region).

The sequential character of these exothermal evolutions under oxidizing conditions became lost with lower air flow rates (Figs. 9 and 10), and the low temperature peak disappeared altogether for gas flow rates of 80 ml min^{-1} (at STP) or less.

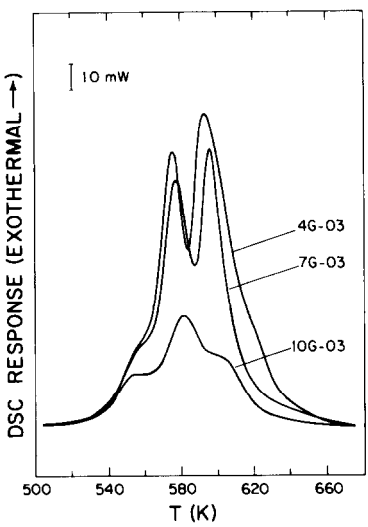

Fig. 8. DSC spectra of the energy evolutions upon thermal decomposition in air (150 ml min^{-1} (at STP), $\beta = 8$ K min^{-1}) of adsorbed amminepalladium complexes on G-03 silica gel versus palladium loading in the DSC crucible normalized to an identical sample mass of 10 mg (high temperature region).

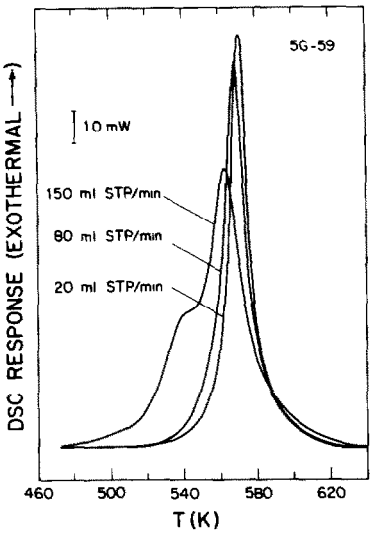

Fig. 9. DSC spectra of the energy evolutions upon thermal decomposition in air ($\beta = 8$ K min^{-1}) of 5G-59 (5.03%Pd w/w) versus gas rate, normalized to an identical sample mass of 10 mg (high temperature region).

Table 5 shows the experimental total enthalpy changes, ΔH_t^A, expressed as kilojoules per mole palladium. These enthalpy changes are somewhat dependent of the amount of palladium loaded on the crucibles and the air flow rate, but they are not substantially different for the macroporous and the microporous silica supports.

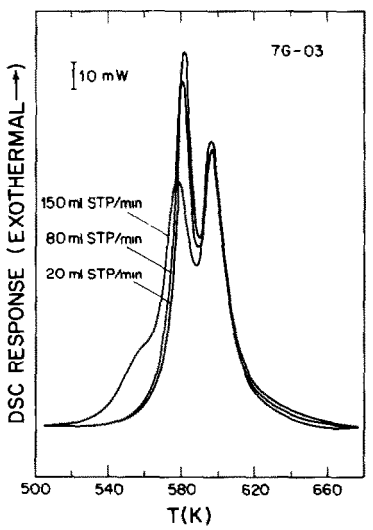

Fig. 10. DSC spectra of the energy evolutions upon thermal decomposition in air ($\beta = 8$ K min^{-1}) of 7G-03 (7.48%Pd w/w) versus gas rate, normalized to an identical sample mass of 10 mg (high temperature region).

TABLE 5

DSC energy evolutions and peak positions upon thermal decomposition in air of amminepalladium complexes ion exchanged on G-59 and G-03 silica gels relative to palladium loading in the DSC chamber and gas flow rate (high temperature region) [a]

Sample code	Air flow rate (ml min^{-1} (at STP))	Sample mass [b] (mg)	Pd loaded in DSC chamber (mmol × 10^3)	Number of DSC peaks	Peak position (K)	Thermal evolution ΔH_t^A (kJ (mol Pd)$^{-1}$)
3G-59	150	10.41	3.37	2	547, 565	−414
5G-59	150	10.78	4.85	2	544, 562	−484
	80	8.78	3.95	1	569	−396
	20	10.04	4.52	1	568	−407
4G-03	150	7.66	2.76	3	557, 582, 602	−411
7G-03	150	7.71	5.04	3	557, 577, 595	−477
	80	7.99	5.23	2	580, 595	−354
	20	7.84	5.13	2	581, 595	−362
10G-03	150	7.97	6.98	3	556, 576, 593	−423

[a] Heating rate, $\beta = 8$ K min^{-1}.
[b] Dry basis.

TABLE 6

DSC energy evolutions and peak positions upon thermal decomposition in air of amminepalladium complexes ion exchanged on G-59 and G-03 silica gels relative to heating rate (high temperature region) [a]

Sample code	Heating rate, β (K min^{-1})	Sample mass [b] (mg)	Pd loaded in the DSC chamber (mmol × 10^3)	Number of DSC peaks	Peak position (K)	Thermal evolution ΔH_t^A (kJ (mol Pd)$^{-1}$)
5G-59	2	8.82	3.97	2	514, 542	−481
	4	10.29	4.63	2	528, 553	−480
	8	10.78	4.85	2	543, 562	−484
	16	10.40	4.68	1	575	−441
	32	10.78	4.85	1	588	−407
7G-03	2	8.25	5.40	3	535, 561, 580	−477
	4	7.65	5.00	3	544, 567, 588	−442
	8	7.71	5.04	3	557, 577, 595	−477
	16	7.92	5.18	2	576, 594	−389
	32	7.78	5.09	2	597, 612	−351

[a] Air flow rate, 150 ml min^{-1} (at STP).
[b] Dry basis.

TABLE 7

Thermogravimetric (TG) weight losses upon thermal decomposition in nitrogen and air of amminepalladium complexes ion exchanged on G-59 and G-03 silica gels (high temperature region) [a]

Sample code	Sample mass [b] (mg)	Pd loaded in the TG chamber (mmol × 10^3)	Atmosphere [c]	Mass loss (mg)			
				Theoretical mass loss per mole Pd for hypothetical freeing of			Experimental values
				$2NH_3$	(NH_3+NH) [d]	$(2NH_3+H_2O)$	
5G-59	33.37	15.0	Air	0.51	0.48	0.78	0.49
	34.43	15.5	N_2	0.53	0.50	0.81	0.52
7G-03	22.88	15.0	Air	0.51	0.48	0.78	0.52
	22.22	14.5	N_2	0.50	0.47	0.75	0.55

[a] Heating rate, $\beta = 6$ K min^{-1}.
[b] Dry basis.
[c] Gas flow rate (N_2 or air): 15 ml min^{-1} (at STP).
[d] (NH_3+NH) stands for $NH_3+0.5N_2+0.5H_2$ (eqn. 5).

DSC spectra were also taken while varying the heating rate, β, between 2 and 32 K min^{-1}, using 5G-59 ($\theta = 0.85$) and 7G-03 ($\theta = 0.70$) with an air flow rate of 150 ml min^{-1} (at STP). As expected, with progressively higher heating rates the exothermal signals merged, into either one (5G-59) or two (7G-03) peaks (Table 6). The low temperature peak disappeared whenever $\beta > 8$ K min^{-1}, with either support type. On the other hand, ΔH_t^A was constant provided $\beta \leq 8$ K min^{-1}, i.e. as long as the consecutive exothermal evolutions were not "forced" to merge.

Thermogravimetric analysis

Table 7 contains the TG results corresponding to the weight losses of 5G-59 and 7G-03 catalysts in the high temperature region upon decomposition under nitrogen and air gas flow (15 ml min^{-1} (at STP)). Together with the experimental values a set of calculated theoretical losses for the following molar ratios is presented (related to the hypothetical loss of ligands and/or their reaction products from the adsorbed complex): $2NH_3$/Pd, $[NH_3 + NH]$/Pd (or more properly: $[NH_3 + 0.5N_2 + 0.5H_2]$/Pd) and $[2NH_3 + H_2O]$/Pd.

The identification of the onset of this high temperature decomposition zone was not straightforward, since the low temperature weight loss extended smoothly up to 500 K. Therefore the experimental values of Table 7 are adequate within an error bounding of about 10–15%.

The comparison of the experimental and theoretical values of the weight losses in this region shown in Table 7 indicates that either $2NH_3$/Pd or $[NH_3 + 0.5N_2 + 0.5H_2]$/Pd are plausible expressions accounting for the loss

of ligands from the palladium complex, the third ($[2NH_3 + H_2O]/Pd$) being an unlikely choice.

X-Ray diffraction

XRD spectra showed that neither Pd^0 nor PdO crystallites of sizeable dimensions, i.e. with diameters larger than 40 Å, were produced after decomposing the *i*G-59 or *i*G-03 catalysts in N_2 or air up to 773 K (gas flow rates = 150 ml min^{-1} (at STP); $\beta = 8$ K min^{-1}).

Non-isothermal kinetic analysis

The rate of irreversible thermal decomposition of a solid can be written as

$$\frac{d\alpha}{dt} = Z \exp(-E_{obs}/RT) f(\alpha) \tag{1}$$

where α is the fraction of solid already decomposed, or conversion; Z is the global pre-exponential factor; E_{obs} is the observable activation energy; R is the gas constant; and $f(\alpha)$ is a function able to express (globally) the type of thermal decomposition involved in the process.

The integration of eqn. (1) for non-isothermal decompositions with linear programming of the temperature, i.e. with $dT/dt = \beta =$ constant, leads to

$$g(\alpha) = \int_0^{\alpha} \left[\frac{d\alpha}{f(\alpha)}\right] = \frac{Z}{\beta} \int_{T_0}^{T} \exp(-E_{obs}/RT)\, dT \tag{2}$$

where T_0 is the temperature for $\alpha = 0$.

Equations (1) or (2) can be used, in principle, to find the kinetic parameters of the decomposition of the amminepalladium complexes under inert (N_2) or oxidizing (air) atmospheres in the high-temperature region. Since different methodologies have been put forward to find those parameters while avoiding the explicit knowledge of $f(\alpha)$ [15], two of them were applied in this work for comparison purposes.

A brief description of these methods together with the results arising from their application to our systems follows now.

Isoconversional method. This method was simultaneously presented by Ozawa [16] and Flynn and Wall [17] to calculate the activation energy E_{obs} of an irreversible decomposition whenever a solid is subjected to a thermal treatment while its temperature is linearly increased. By using Doyle's approximation [18] to solve the second integral in eqn. (2) these authors obtained a new expression

$$\ln \beta = \ln\left[\frac{ZE_{obs}}{Rg(\alpha)}\right] - 5.3305 - 1.0527\left[\frac{E_{obs}}{RT_\alpha}\right] \tag{3}$$

where T_α is the temperature at which a certain fraction α of the solid is decomposed or converted.

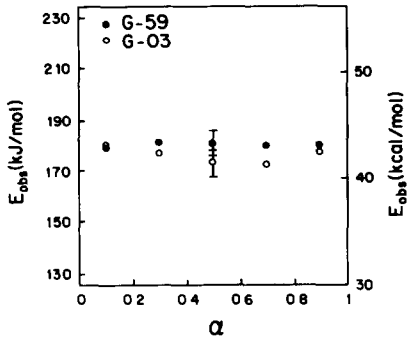

Fig. 11. Calculated values of the activation energies ($E_{obs.}$) versus fractional conversion (α) using Ozawa's method [16], for the decomposition in nitrogen ($\beta \leq 32$ K min^{-1}) of adsorbed amminepalladium complexes on G-59 and G-03 silica gels.

Because α is proportional to the fractional area under the decomposition curve given by any suitable technique, DSC spectra allowed us to calculate E_{obs} versus α by varying the heating rate (β) because ln β is proportional to $1/T_\alpha$ (eqn. 3). This is why the method is called "isoconversional". Then, if $g(\alpha)$ does not change for different conversion levels, i.e. if there are no interactions among decomposing species, E_{obs} will be the same for any value of α.

Obviously, this method is only applicable for singly peaked thermal evolutions and thus it was only used to evaluate data taken from the decompositions in nitrogen.

Figure 11 shows the results obtained after using this method to analyze the decompositions of 5G-59 and 7G-03 under N_2 flow. Only data for $\beta \leqslant 32$ K min^{-1} (i.e. where ΔH_t^N was constant) were used to perform the calculations. It is apparent that $E_{obs}^{5G\text{-}59}$ and $E_{obs}^{7G\text{-}03}$ are both independent of the conversion level and identical, within the calculated error bounds shown in the figure. The averaged values for each sample were 180 ± 5 kJ (mol Pd)$^{-1}$ (43.0 ± 1.2 kcal mol^{-1}) and 176 ± 5 kJ (mol Pd)$^{-1}$ (42.1 ± 1.2 kcal mol^{-1}) respectively.

Peak temperature method. This method calculates E_{obs} and Z by using a relationship between the value of the temperature at the peak maximum (T_p) and the heating rate (β) originally found by Kisinger [19]

$$\ln\left[\frac{\beta}{T_p^2}\right] = \ln\left[\frac{ZR}{E_{obs}}\right] - \left[\frac{E_{obs}}{RT_p}\right] \tag{4}$$

The kinetic parameters can be calculated from the values of the slope and the intercept with the ordinate axis in the linear regression of $\ln[\beta/T_p^2]$ versus $1/T_p$. The peak temperature method has also been used in temperature programmed desorption (TPD) and temperature programmed reaction (TPR) experiments, as applied to the study of supported metals [20–22].

TABLE 8

DSC non-isothermal kinetic analysis (Kisinger's method [19]): values of the activation energy, E_{obs}, and global frequency factor, Z, for the decomposition in nitrogen and air of amminepalladium complexes ion exchanged on G-59 and G-03 silica gels in the high temperature region

Sample code	Atmosphere [a]	Peak order	Heating rate, β (K min^{-1})	Kinetic parameters		Linear correlation coefficient
				$E_{obs.}$ (kJ mol^{-1})	Z (s^{-1})	
5G-59	Air	1st	2, 4, 8	97.8	7.9×10^{08}	1.000
		2nd	2, 4, 8	161.3	4.6×10^{14}	0.995
	N_2		4, 8, 16, 32	182.0	2.3×10^{13}	0.994
7G-03	N_2		4, 8, 16, 32	173.8	1.1×10^{13}	0.999

[a] Gas flow rate: 150 ml min^{-1} (at STP).

The method was used here to calculate the kinetic parameters of the thermal decomposition of the amminepalladium complexes in 5G-59 and 7G-03 under nitrogen by resorting to experimental data for which ΔH_t^N was constant ($\beta \leqslant 32$ K min^{-1}).

Likewise, DSC results for the thermal decomposition of 5G-59 under air ($\beta \leqslant 8$ K min^{-1}) at constant ΔH_t^A were employed. It was impossible to apply it to the decomposition of 7G-03 in an oxidative atmosphere, as discussed below in more detail.

Table 8 summarizes the results of these calculations. The close agreement between the values of the activation energies (E_{obs}) for the decomposition of the complex under inert atmosphere calculated with this method and those obtained via the former procedure (the isoconversional technique) is remarkable.

X-Ray photoelectron spectroscopy

XPS spectra taken from the 5G-59 and 7G-03 catalysts samples are shown in Fig. 12. Table 9 details the binding energies (BE) and the full width at half maximum (FWHM) of these peaks, as well as those corresponding to Pd foil and bulk PdO. Since the differences in binding energies between the $3d_{5/2}$ and $3d_{3/2}$ signals was always about the same (5.1–5.3 eV), only the features corresponding to the former XPS peaks are reported.

The hydrogen reduced 7G-03 catalyst as well as the nitrogen decomposed samples (5G-59 and 7G-03) showed about the same values of the Pd $3d_{5/2}$ BE. The reduction procedure on 7G-03 left only highly dispersed palladium metal crystallites on the surface, which was confirmed by us by electron microscopy and H_2 chemisorption [24].

It is well known that Pd^0 BE values larger than that of bulk metal are obtained on inert supports whenever metal crystallites smaller than about 40–50 Å are formed on the said surfaces [25–28]. Moreover, palladium

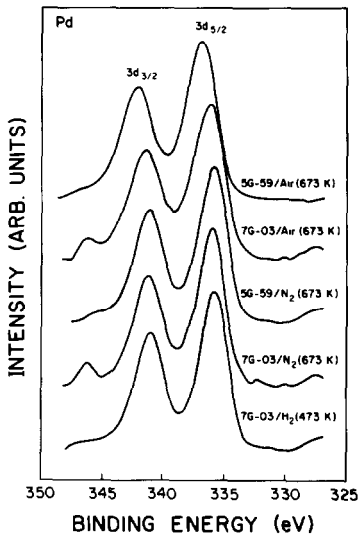

Fig. 12. XPS spectra of Pd $3d_{5/2}$ and $3d_{3/2}$ signals corresponding to precursors of Pd/SiO_2 catalysts (amminepalladium complexes ion exchanged on G-59 and G-03 silica gels) upon exposure to oxidizing, inert or reducing atmospheres.

metal crystallites on the surfaces of hydrogen reduced catalysts have been shown not to redisperse [24] nor reoxidize upon exposure to air at ambient conditions [29,30].

Thus, the Pd $3d_{5/2}$ BE value from the 7G-03/H_2 sample corresponds to well dispersed Pd^0, probably with weakly chemisorbed surface oxygen [23].

TABLE 9

Binding energy (BE) values and full width at half maximum (FWHM) of Pd $3d_{5/2}$ XPS peaks corresponding to precursors of Pd/SiO_2 catalysts (amminepalladium complexes ion exchanged on G-59 and G-03 silica gels) upon exposure to oxidizing, inert or reducing atmospheres

Sample code	Atmosphere	Maximum temperature (K)	Pd $3d_{5/2}$ peak features	
			BE [a] (eV)	FWMH (eV)
7G-03	H_2	473	335.8	2.8
	N_2	673	336.0	2.8
	Air	673	336.3	3.3
5G-59	N_2	673	335.9	2.8
	Air	673	336.9	2.7
Pd foil			335.2 [b]	
PdO			336.5 [b]	

[a] Peak positions are referenced to Si 2p = 103.2 eV.
[b] After ref. 23, when referenced to C 1s = 284.6 eV.

Also, within experimental error, it is to be concluded that the decomposition process with nitrogen left only (ultradispersed) palladium metal crystallites on both 5G-59 and 7G-03.

The air decomposed catalyst showed distinctive, significantly higher binding energies. On the microporous G-03 support the average BE (336.3 eV) was slightly under the value of bulk PdO (336.5 eV), but the width of the signal (FWHM = 3.3 eV) indicates that the decomposition of the ammine-palladium complex left at least two different surface species, probably a mixture of Pd^0 and $[(SiO)_2]^{2-}Pd^{2+}$.

Conversely, on the macroporous 5G-59 catalyst a fully oxidized surface is left upon exposure to an air flow at 673 K, probably with strong surface bonding of surface Pd^{2+} cations coordinated to lattice oxygen. Strong surface bonding of surface Pd^{2+} cations coordinated to lattice oxygen has

TABLE 10

Estimated percentage of remaining ammine ligands and optical appearance of precursors of Pd/SiO_2 catalysts (amminepalladium complexes ion exchanged on G-59 and G-03 silica gels) upon exposure to oxidizing, inert or reducing atmospheres

Sample code	Atmosphere	Maximum temperature (K)	Remaining NH_3 ligands (%)	Final color	Ref. [a]
5G-59	Air	298	100	White	
		393	50	Yellow	
		723	0	Red-brown	
	N_2	723	0	Black	
	H_2	723 [b]	0	Black	
		723 [c]	0	Black	
7G-03	Air	298	100	White	
		393	50–70	Yellow	
		723	0	Brown	
	N_2	723	0	Black	
	H_2	723 [b]	0	Black	
		723 [c]	0	Black	
	He	623	0	Black	
$Pd(NH_3)_4(NO_3)_2$			100	White	11
$Pd(NH_3)_4Cl_2 \cdot H_2O$			100	Colorless	32
$Pd(NH_3)_2(OH)_2$			50	Yellow	11
$Pd(NH_3)_2Cl_2$			50	Yellow	32
$PdO \cdot xH_2O$			0	Yellow-brown	11
$PdO_2 \cdot xH_2O$			0	Red	32

[a] This work unless otherwise stated.

[b] H_2 reduced (2 h), uncalcined sample.

[c] H_2 reduced (2 h), after previous calcination in air at 723 K.

been shown to give even larger Pd $3d_{5/2}$ BE values than those of bulk PdO by Vedrine et al. [31]. When these authors decomposed $[Pd(NH_3)_4]^{2+}$/zeolite in O_2 at 773 K they found palladium BE values of 339.4 eV.

Table 10 summarizes several of the thermal decomposition results, obtained under different conditions, and includes optical characteristics of various palladium complexes for further discussion below.

DISCUSSION

Drying—low-temperature thermal decomposition

As already stated, ion exchange of amminepalladium complexes prepared from palladium acetate in aqueous alkaline solutions (pH $\geqslant$ 10.5) results in the adsorption of tetramminepalladium on gels of silica without substitution of NH_3 ligands in the coordination sphere of the Pd^{2+} cations [3] (formally, $[Pd(NH_3)_4]^{2+}$ $[(SiO)_2]^{2-}$; hereafter TPSiO).

DRS spectra corresponding to the different drying procedures at 313 K of 2G-59 and 2G-03 show that after these dryings a progressive substitution of the NH_3 ligands by surface water occurs, and the longer the drying period the more extensive this substitution. Moreover, from DRS spectra the assignment of this progressive substitution of ligands to a final total of two exchanged NH_3 after drying the 2G-59 samples with forced convection of air at 393 K for 2 h is straightforward (Fig. 1). The diaquo-diamminepalladium complex, $[Pd(NH_3)_2(H_2O)_2]^{2+}$, is the most likely ending surface species regardless of the pH of the washing procedures or the previous drying types under the moderate conditions to which the solid was subjected. Either due to the use of gas chromatography grade air without water traps or because the catalyst pellets were exposed to atmospheric conditions prior to obtaining the DRS spectra this inference is immediate.

Longer drying periods at 393 K are required for the 2G-03 catalyst to complete this ligand substitution. Thermal decomposition results in the low-temperature region showing more directly (Fig. 4) that the freeing of NH_3 ligands on 2G-03 is certainly more difficult than on 2G-59.

In previous work [3] we have shown that, whereas both silicas are chemically equivalent, they have widely different structures. G-59 is a macroporous silica gel but G-03 is a microporous solid so that the resulting palladium surface complex on the latter support after a drying period of 2 h (393 K) is then $[Pd(NH_3)_n(H_2O)_{4-n}]^{2+}$, with $2 < n < 3$. In this regard our results keep close agreement with those of Gubitosa et al. [4], who adsorbed $[Pd(NH_3)_4](OH)_2$ on microporous silica in NH_4OH(aq) and dried their samples in air at 383 K. Their chemical analysis of the further direct reduction with H_2 of the residual surface ammonia gave a calculated NH_3 to Pd molar ratio averaging 2.65.

Other supported metal complexes have been shown to follow similar ligand exchange pathways after drying: Olivier et al. [33] reported that

$[Ni(NH_3)_6]^{2+}$ adsorbed onto silica as $[Ni(NH_3)_4]^{2+}[(SiO)_2]^{2-}$ ends up as a diaquo-diammine nickel complex $[Ni(NH_3)_2(H_2O)_2]^{2+}$ upon stove drying (353 K) followed by rehydration in atmospheric conditions. Likewise, Amara et al. [7] adsorbed $[Cu(NH_3)_4]^{2+}$ on a gel of silica obtaining a tetrammine surface complex which became again a substituted diaquo-diammine species after overnight drying at 353 K.

Olivier's group also showed that the dehydration of adsorbed aquo-ammine nickel complexes manifests itself by a shift in the absorption maxima towards longer wavelengths of approximately 15 nm whenever a H_2O ligand is substituted by a $(SiO)^-$ [33]. If that had been the case for our amminepalladium complexes, we would have found absorption maxima around 370 nm were the surface species $[Pd(NH_3)_2]^{2+}[(SiO)_2]^{2-}$, which was certainly not observed in the DRS spectra.

Similarly the substitution of a single water molecule by $(SiO)^-$, which would imply absorption maxima at about 356 nm, is discarded altogether.

Thus, if prior to the spectroscopic scans the solid pellets are exposed to atmospheric conditions, diaquo-diamminepalladium complex is the most likely surface species observable by DRS after drying at 393 K in "regular" air on these gels of silica, with longer drying times required when the microporous support G-03 is used.

It is only possible to obtain "bare" surface diamminepalladium (formally, $[Pd(NH_3)_2]^{2+}[(SiO)_2]^{2-}$; hereafter DPSiO) whenever dry nitrogen or air are used (in a closed enclosure) to decompose TPSiO. This is confirmed by the mass balances obtained from our TG results, performed in the high-temperature decomposition region (Table 7), as discussed in more detail below.

High-temperature thermal decomposition

Inert atmosphere

Combined DSC and thermogravimetric results (Figs. 5 and 6, Table 7) allows us to state that the decomposition of DPSiO in nitrogen occurs below 630–640 K, (i) with loss of two NH_3 ligands, and (ii) without surface dehydration of the gels of silica themselves, at least within the detection limits of these techniques. Therefore, either Pd^{2+} ions and/or Pd^0 crystallites are left on the silica surfaces after the high-temperature thermal treatment.

Earlier works have shown that when $[Pd(NH_3)_4]^{2+}$ complexes adsorbed onto zeolites are thermally decomposed in He [10] or Ar [34] they self decompose, and only palladium metal is left on the surface.

In contrast, bulk thermal decomposition experiments of $Pd(NH_3)_4X_2$ (X = Cl, Br, I) in a cross flow of He [13] have shown that, (i) tetramminepalladium halides free two of the NH_3 ligands in a first stage, yielding *trans*-$X_2Pd(NH_3)_2$; (ii) these trans complexes decompose in a different fashion, according to the nature of X, such that if X = Cl, Pd^{2+} wholly

reduces to Pd^0; if X = Br, a mixture of $PdBr_2$ and Pd^0 is obtained (with a Pd^{2+}/Pd^0 molar ratio of 4); and if X = I, only PdI_2 is produced.

The polarizability of halide anions follows the sequence $Cl^- < Br^- < I^-$. Therefore, the less polarizable the anion in a palladium halide the higher the feasibility of reduction of Pd^{2+} to palladium metal by the NH_3 ligands.

From these observations, surface oxygen anions pertaining to the siloxy functional groups $(SiO)^-$ being less polarizable than Cl^-, it is reasonable to think that in the absence of O_2 the $[Pd(NH_3)_2]^{2+}[(SiO)_2]^{2-}$ complex decomposes leaving Pd^0 on the surface of silica gels, such as has been observed in zeolites [9,10]. By adding to this reasoning the TG-derived mass balance and DRS data summarized in Table 10, and our XPS results, it has to be concluded that the Pd^{2+} cations are reduced to palladium metal crystallites by the NH_3 ligands set free during the thermal decomposition in inert atmosphere.

We tend to dismiss the proposition of Spector et al. [8] about –OH surface groups being responsible for the said surface reduction for two reasons. Firstly our TG mass balance rules out the possibility of having a simultaneous freeing of surface NH_3 and H_2O and, secondly it is utterly impossible to have the single evolution of water instead of NH_3 because silica gels do not retain NH_3 any longer at these high temperatures.

The following single equation should then suffice to describe the whole high temperature decomposition process under nitrogen

$$[(SiO)_2]^{2+}[Pd(NH_3)_2]^{2+} \rightarrow Pd^0 + 2SiOH + 0.5N_2 + 0.5H_2 + NH_3 \qquad (5)$$

However, the calculated decomposition enthalpies, ΔH_t^N (kJ (mol Pd)$^{-1}$) were not equal for the two supported catalysts (Table 4). A possible reason for these dissimilar enthalpy values could be related to the simultaneous occurrence of the well-documented dissociative catalytic decomposition of NH_3 on transition metals, such as Pt [35–40], Ni [41–43] or Pd [44]. Because G-03 has a microporous structure it is then feasible that the catalytic decomposition on Pd^0 crystallites of the ammonia ligands is more extensive than on G-59.

That being the picture, when the (average) experimental difference of the ΔH_t^N between both supports (39.1 kJ (mol Pd)$^{-1}$; see Table 4, $\beta \leqslant 32$ K min^{-1}) and the tabulated value of the enthalpy of formation of ammonia (-50.8 kJ mol^{-1} [45]) are brought into consideration, two extreme alternatives concerning the decomposition of the freed NH_3 ligand remain. Either all the NH_3 decomposes whenever the support is G-03, and then on G-59 the decomposed fraction (ξ) is (approximately) 0.23, or when the support is G-59 NH_3 does not decompose and then on G-03 $\xi \approx 0.77$.

Thus, the following comprehensive equation results

$$[(SiO)_2]^{2+}[Pd(NH_3)_2]^{2+} \rightarrow Pd^0 + 2SiOH + \frac{1+\xi}{2}N_2 + \frac{1+3\xi}{2}H_2 + (1-\xi)NH_3 \qquad (6)$$

where $\xi \leqslant 0.23$ for Pd/5G-59 and/or $\xi \geqslant 0.77$ for Pd/7G-03.

Considering that only about 23% of the decomposed NH_3 can be converted into N_2 and H_2 on Pd/5G-59, the calculated total enthalpy change for the reaction indicated by eqn. (5) becomes

$$\Delta H^{N}_{DPSiO} = 32.3 \pm 4.2 \text{ kJ (mol Pd)}^{-1} \qquad (7.7 \pm 1.0 \text{ kcal (mol Pd)}^{-1})$$

The DSC spectra themselves shed additional light on the kinetics of the combined decomposition of the amminepalladium complex and the evolved ammonia because, (i) if the rate of the catalytic decomposition of NH_3 on the newly formed Pd^0 crystallites were greater than the rate of decomposition of the DPSiO complex (eqn. (5)) only the latter process could be "seen" in the DSC spectra, whereas (ii) if the opposite were true another DSC peak or shoulder would appear, at least at the lower heating rates (β) on 7G-03, or the DSC signals from 7G-03 would have minima at higher temperatures than those from 5G-59. Certainly the former situation applies (Figs. 5 and 6).

Then, as the observable kinetics are those of a rate process singly related to the decomposition of DPSiO (eqn. 5), the same value of the activation energy (E_{obs}) and the pre-exponential factor (Z), should be found at any level of decomposition of the complex (α) on either of the silica supports. This assertion is reasonably well supported by our experimental data, as shown in Fig. 11 and Table 8, so that the (averaged) kinetic parameters for the decomposition of DPSiO in nitrogen are $E^{N}_{DPSiO} = 181$ kJ (mol Pd)$^{-1}$ and $Z^{N}_{DPSiO} = 2.3 \times 10^{13}$.

Oxidizing atmosphere

The interpretation of these DSC and TG experiments is more complex than the one given above to rationalize the decomposition of DPSiO under nitrogen. These data indicate that under oxidizing conditions the decomposition of DPSiO occurs (i) with loss of two ammonia ligands per Pd atom; (ii) with highly exothermal evolutions, which induces one into thinking of concomitant oxidation of NH_3 with consequent production of H_2O; (iii) at least in two consecutive stages; and (iv) at lower temperatures than in inert atmosphere.

XPS results, as well as those of Table 10, show qualitatively that the supported palladium complex becomes partially or completely oxidized after the decomposition on either support. Because no endothermal DSC signal was put into evidence while decomposing DPSiO on 5G-59 we think that on this support all of the palladium is Pd^{2+} at the end of the high temperature decomposition. However, in the case of the microporous 7G-03 diffusional hindrances hamper the total decomposition of NH_3, as discussed below.

Because ΔH^{A}_{t} values varied somewhat with the Pd loading ($\pm 5\%$), and also with the air flow rate, only qualitative hypotheses will be put forward hereafter as related to this *i*G-03 system.

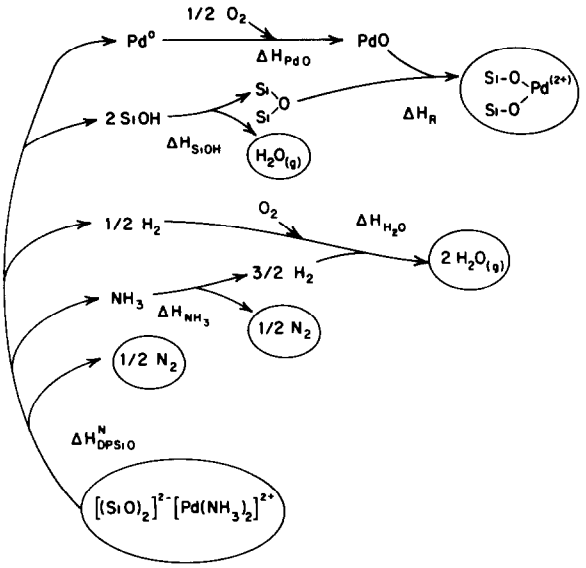

ΔH	(KJ/mol)	Ref
ΔH^{N}_{DPSiO}	32 2	This work
$\Delta H^{553\,K}_{PdO}$	-74 5	[32]
ΔH_{SiOH}	17 5	[46]
$\Delta H^{553\,K}_{H_2O}$	244 5	[45,47]
$\Delta H^{553\,K}_{NH_3}$	-50 2	[45]

Fig. 13. Schematic representation of the decomposition of DPSiO under inert and oxidizing atmospheres.

Taking the 5G-59 data first, since the decomposition of NH_3 produces hydrogen, the exothermal DSC peaks are to be assigned to the production of H_2O (given the fast reactivity of H_2 with O_2). Assuming all the NH_3 decomposes in air to give N_2 and H_2O [10,34] we can write the representative equation

$$[(SiO)_2]^{2-}[Pd(NH_3)_2]^{2+} + 1.5O_2 \rightarrow [(SiO)_2]^{2-}(Pd)^{2+} + N_2 + 3H_2O \qquad (7)$$

Using the thermodynamic cycle pictured in Fig. 13, the total enthalpy change, ΔH^{A}_{DPSiO}, can be estimated as

$$\Delta H^{A}_{DPSiO} = \Delta H^{N}_{DPSiO} + \Delta H_{PdO} + \Delta H_{SiOH} + \Delta H_R + 2\Delta H_{H_2O} - \Delta H_{NH_3} \qquad (8)$$

where ΔH^{N}_{DPSiO} is the enthalpy of decomposition of DPSiO in N_2, ΔH_{PdO} is the heat of formation of $PdO_{(s)}$, ΔH_{SiOH} is the enthalpy of surface dehydration of amorphous silica per mol H_2O, ΔH_R is the enthalpy of bond rearrangements (Fig. 13), ΔH_{H_2O} is the heat of formation of $H_2O_{(g)}$, and ΔH_{NH_3} is the heat of formation of $NH_{3(g)}$.

The estimation of ΔH^{A}_{DPSiO} is made by further assuming that (a) ΔH^{N}_{DPSiO} and ΔH_{SiOH} are temperature independent (thus, our own ΔH^{N}_{DPSiO} experimental value obtained from the DPSiO decomposition under nitrogen, and an averaged ΔH_{SiOH} value from the DSC data of Sharpataya et al. [46] were used), (b) $\Delta H_R \approx 0$ kJ mol^{-1}, these being only internal bond rearrangements, and (c) the values of ΔH_{PdO}, ΔH_{H_2O} and ΔH_{NH_3}, calculated at the average of the peak temperatures (553 K) are representative.

Figure 13 includes the complete set of enthalpy values together with their corresponding references.

The experimental value of ΔH^{A}_{DPSiO}, as taken from the average of the decomposition data of DPSiO on 5G-59 (Table 6, $\beta \leqslant 8$ K min^{-1}) is -482 kJ (mol Pd)$^{-1}$ (-115 kcal (mol Pd)$^{-1}$). The corresponding enthalpy value, calculated as per eqn. (7) using the above-mentioned estimates, was -463 kJ (mol Pd)$^{-1}$ (-111 kcal (mol Pd)$^{-1}$), which is within 4% of the experimentally obtained figure.

We think it unfeasible that nitrogen oxides might be formed during the decomposition process for two reasons: firstly, the formation of all of these oxides is endothermal, which would imply the obtainment of a larger estimate, far from the experimental value, of ΔH^{A}_{DPSiO}, and secondly, the mass spectra taken by Exner et al. [34] during the decomposition of $[Pd(NH_3)_4]^{2+}$/zeolites in oxygen have not revealed the presence of any of these nitrogen oxides.

The global reaction occurring upon the decomposition in air of DPSiO/5G-59 is then that indicated in eqn. (7). However, the DSC spectra show that at least two consecutive stages are present. We suggest that these stages are the loss and fast decomposition of a first NH_3 ligand

$$[(SiO)_2]^{2-}[Pd(NH_3)_2]^{2+} + 0.75O_2 \rightarrow [(SiO)_2]^{2-}(Pd)^{2+} \cdots NH_3 + 0.5N_2 + 1.5H_2O \quad (7a)$$

followed by thermal activation and decomposition of the remaining ligand from the less unstable $[(SiO)_2]^{2-}(Pd)^{2+} \cdots NH_3$ surface species, whose detachment should presumably have a higher activation energy such that a second, resolved DSC peak appears under suitable heating rates

$$[(SiO)_2]^{2-}(Pd)^{2+} \cdots NH_3 + 0.75O_2 \rightarrow [(SiO)_2]^{2-}(Pd)^{2+} + 0.5N_2 + 1.5H_2O \quad (7b)$$

Using again thermodynamic cycles, the calculated enthalpy changes for reactions (7a) and (7b) were -147 and -317 kJ (mol Pd)$^{-1}$ (-35.1 and -75.6 kcal (mol Pd)$^{-1}$), respectively (i.e. the estimated ratio $\Delta H_{7b}/\Delta H_{7a} = 2.2$).

TABLE 11

DSC peak heights ratios corresponding to the decomposition in air, in the high temperature region, of precursors of Pd/SiO_2 catalysts (amminepalladium complexes ion exchanged on G-59 silica gel) [a]

Sample code	Heating rate, β (K min^{-1})	Peak height ratio (2nd/1st)
5G-59	2	1.7
	4	2.0
	8	2.1

[a] Air flow rate, 150 ml min^{-1} (at STP).

From Table 11 it is seen that the height ratio between the second and the first exothermal DSC peaks is about 2, in reasonably good agreement with the calculated ratio. Therefore the values of the kinetic parameters of each of the consecutive decompositions obtained using the peak temperature method (Table 8) should indeed correspond to reactions (7a) and (7b).

Next, the high temperature decomposition in air of DPSiO on *i*G-03 will be analyzed. As already stated, complex diffusional hindrances are supposed to hamper straight-cut answers. Therefore, it is to be expected that the ion-exchanged palladium complexes deposited inside the narrow pores of this microporous silica would decompose at apparently higher peak temperatures.

Moreover, the thermal decomposition inside these narrow pores has to be quite similar to that under inert atmosphere, i.e. with Pd reduction caused by part of the H_2 produced by the decomposition of NH_3 ligands, the rest of the produced hydrogen then reacting with air from the outside atmosphere while counterdiffusing to the pore mouths. Coupled endothermal and exothermal processes would then be convoluted into the DSC spectra giving rise to a "third" peak.

These second and third peaks cannot correspond to consecutive steps of nitrogen oxidation, because they do not tend to coalesce when the heating rate, β, is increased. Furthermore, the valley between them is located in the same temperature region where DPSiO decomposes under inert conditions.

In consequence, and bringing in the conclusive XPS results (Fig. 12 and Table 9), we support the hypothesis of palladium being partially reduced on 7G-03. Then, the thermodynamic cycle depicted in Fig. 13 would still be representative of the complete process, under the condition that merely a fraction (ϕ) of the palladium total be allowed to oxidize. So, to estimate the total enthalpy change of the decomposition of DPSiO on 7G-03 in air (ΔH^{A}_{DPSiO}) we can now write

$$\Delta H^{A}_{DPSiO} = \Delta H^{N}_{DPSiO} + \phi\Delta H_{PdO} + \phi\Delta H_{SiOH} + \phi\Delta H_{R} + 2\Delta H_{H_2O} - \Delta H_{NH_3} \tag{9}$$

where ϕ is the fraction of PdO formed and $(1-\phi)$ is that of Pd^0.

Lastly, if ϕ were proportional to the height of the first DSC peak, which corresponds to the exothermal decomposition process represented by eqn. (7a), the ratio of peak heights at high air flow rates between the signals from 7G-03 and 5G-59 samples (normalized per mol of Pd) would roughly indicate the fraction of Pd^{2+} formed on 7G-03, because on 5G-59 all of the palladium is oxidized to Pd^{2+} (Fig. 12). Table 12 shows that $\phi \approx 0.6$, i.e. that about 40% of the palladium would become reduced on 7G-03. Using this ϕ value in eqn. (9) gives a calculated total enthalpy change $\Delta H^{A}_{DPSiO} = -441$ kJ (mol Pd)$^{-1}$ (-105 kcal (mol Pd)$^{-1}$), which is just 5% smaller than the experimental value (-465 kJ (mol Pd)$^{-1}$). Coincidently, Reagan et al.

TABLE 12

Peak height ratios of the first DSC signals corresponding to the decomposition in air, in the high temperature region, of precursors of Pd/SiO_2 catalysts (amminepalladium complexes ion exchanged on G-03 and G-59 silica gels) [a]

Heating rate, β (K min^{-1})	Peak height ratios (1st peak) 7G-03/5G-59 [b]
2	0.5
4	0.6
8	0.6

[a] Air flow rate, 150 ml min^{-1} (at STP).
[b] Each peak height normalized per mol of Pd in the crucible.

[10] found about the same proportion of reduced palladium (30% mol mol^{-1}) after decomposing $[Pd(NH_3)_4]^{2+}$ in air on zeolites.

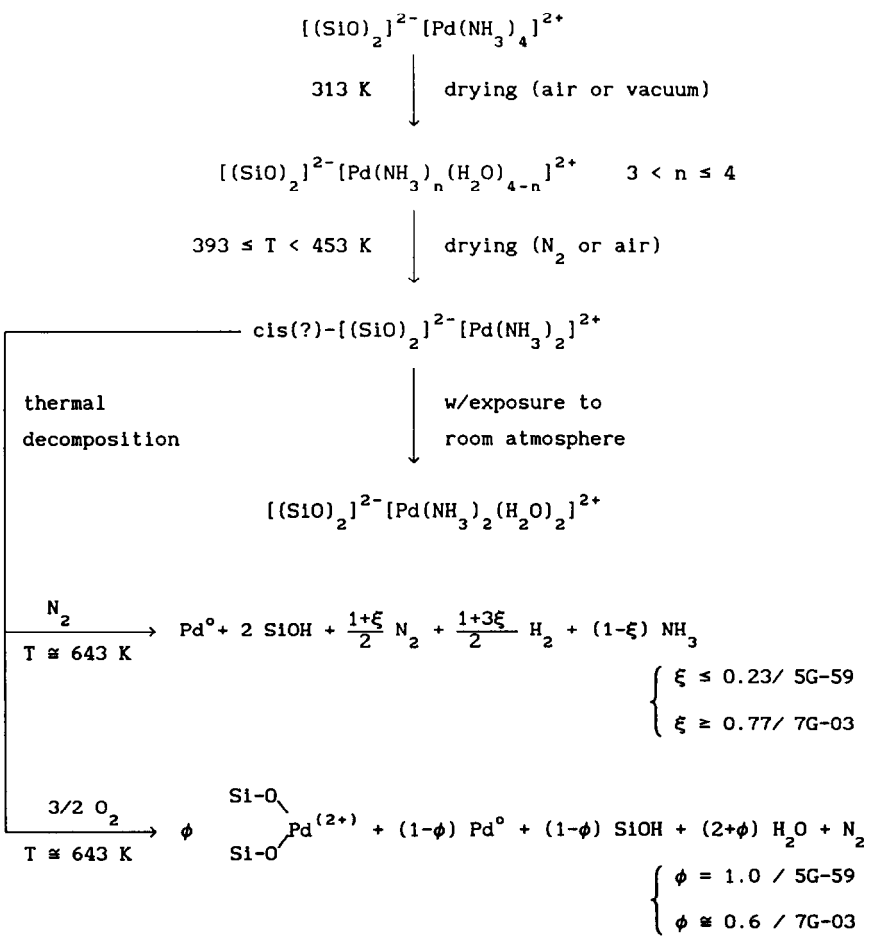

Scheme 1.

Summing up, Scheme 1 describes at a glance the complete drying-calcining evolution of the silica supported tetramminepalladium complex.

ACKNOWLEDGMENTS

Thanks are given to José L. Giombi and José L. Castañeda for technical assistance, and to Prof. Cristina E. González for her help in revising the English version of the manuscript. DAREX S.A.I.C. kindly provided the Davison silica gels. We acknowledge the financial aid received from the National Council of Scientific and Technical Research of Argentina (CONICET) and from Universidad Nacional del Litoral (Santa Fe, Argentina).

REFERENCES

1 B. Delmon and M. Houalla, in B. Delmon, P. Grange, P. Jacobs and G. Poncelet (Eds.), Preparation of Catalysts, Vol. 2, Elsevier, Amsterdam, 1979, p. 439.
2 J.W. Gues, in G. Poncelet, P. Grange and P.A. Jacobs (Eds.), Preparation of Catalysts, Vol. 3, Elsevier, Amsterdam, 1983, p. 1.
3 A.L. Bonivardi and M.A. Baltanás, J. Catal., 125 (1990) 243.
4 G. Gubitosa, A. Berton, M. Camia and N. Pernicone, in G. Poncelet, P. Grange and P.A. Jacobs (Eds.), Preparation of Catalysts, Vol. 3, Elsevier, Amsterdam, 1983, p. 431.
5 M.A. Kohler, J.C. Lee, D.L. Trimm, N.W. Cant and M.S. Wainwright, Appl. Catal., 31 (1987) 309.
6 J.C. Lee, D.L. Trimm, M.A. Kohler, M.S. Wainwright and N.W. Cant, Catal. Today, 2 (1988) 643.
7 M. Amara, M. Bettahar, L. Gengembre and D. Olivier, Appl. Catal., 35 (1987) 153.
8 G. Spector, M. Briend and D. Delafosse, J. Chim. Phys., 22 (1985) 449.
9 R.A. Dalla Betta and M. Boudart, Proc. 5th Int. Congr. Catalysis, Vol. 2, North Holland, Amsterdam, 1973, p. 1329.
10 W.J. Reagan, A.W. Chester and G.T. Kerr, J. Catal., 69 (1981) 89.
11 S.T. Homeyer and W.M.H. Sachtler, J. Catal., 117 (1989) 91.
12 S.T. Homeyer and W.M.H. Sachtler, J. Catal., 118 (1989) 266.
13 W.W. Wendlandt and L.A. Funes, J. Inorg. Nucl. Chem., 26 (1964) 1879.
14 T.H. Fleisch, R.F. Hicks and A.T. Bell, J. Catal., 87 (1984) 398.
15 E. Koch, Non-Isothermal Reaction Analysis, Academic Press, London, 1977.
16 T. Ozawa, Bull. Chem. Soc. Jpn., 38 (1965) 1881; J. Therm. Anal., 2 (1970) 301.
17 J.H. Flynn and L.A. Wall, Polym. Lett., 4 (1966) 323.
18 C.D. Doyle, J. Appl. Polym. Sci., 6 (1962) 639.
19 H.E. Kisinger, J. Res. Nat. Bur. Stand., 57 (1956) 217; Anal. Chem., 29 (1957) 1702.
20 J.L. Falconer and J.A. Schwarz, Catal. Rev. Sci. Eng., 25 (1983) 141.
21 R.P.H. Gasser, An Introduction to Chemisorption and Catalysis by Metals, Oxford Scientific, Oxford, 1985.
22 P. Forzatti, E. Tronconi and L. Lietti, in N.P. Cheremisinoff (Ed.), Handbook of Heat and Mass Transfer, Vol. 3, Gulf Publishing, Houston, 1989, Chapter 8.
23 K.S. Kim, A.F. Gossmann and N. Winograd, Anal. Chem., 46 (1974) 197.
24 (a) A.L. Bonivardi and M.A. Baltanás, J. Catal., in press.
(b) A.L. Bonivardi, Ph.D. Thesis, Universidad National del Litoral, Argentina, 1991.
25 Y. Takasu, R. Unwin, B. Tesche and A.M. Bradshaw, Surf. Sci., 77 (1978) 219.
26 Yu.A. Ryndin, L.V. Nosova, A.I. Boronin and A.L. Chuvilin, Appl. Catal., 42 (1988) 131.

27 M.G. Mason, Phys. Rev. B, 27 (1983) 748.
28 S. Kohiki, Appl. Surf. Sci., 25 (1986) 81.
29 V. Pitchon, M. Guenin and H. Praliaud, Appl. Catal., 63 (1990) 333.
30 L.S. Shyu, K. Otto, W.L.H. Watkins, G.W. Graham, R.F. Belitz and H.S. Gandhi, J. Catal., 114 (1988) 23.
31 J.C. Vedrine, M. Dufaux, C. Naccache and B. Imelik, J. Chem. Soc., Faraday Trans. 1, 74 (1978) 440.
32 R.C. Weats (Ed.), Handbook of Chemistry and Physics, 67th Edn., CRC Press, FL, 1986.
33 D. Olivier, L. Bonneviot, F.X. Cai, M. Che, P. Gihr, M. Kermarec, C. Lepetit-Pourcelot and B. Morin, Bull. Soc. Chim. Fr., 3 (1985) 370.
34 D. Exner, N. Jaeger, K. Möller and G. Schulz-Ekloff, J. Chem. Soc., Faraday Trans. 1, 78 (1982) 3537.
35 W.L. Guthrie, J.D. Sokol and G.A. Somorjai, Surf. Sci., 109 (1981) 390.
36 J.L. Gland, Surf. Sci., 71 (1978) 327.
37 J.L. Gland and E.B. Kollin, J. Vac. Sci. Technol., 18 (1981) 604.
38 J.L. Gland and E.B. Kollin, Surf. Sci., 104 (1981) 478.
39 D.G. Löffler and L.D. Schmidt, J. Catal., 41 (1976) 440.
40 W. Liu and T.T. Tsong, Surf. Sci., 165 (1986) L26.
41 M. Hüttinger and J. Küppers, Surf. Sci., 130 (1983) L277.
42 M. Grunze, M. Golze, R.K. Driscoll and P.A. Dowben, J. Vac. Sci. Technol., 18 (1981) 611.
43 G. Ertl and J. Rüstig, Surf. Sci., 119 (1982) L314.
44 K. Kunimori, T. Kawai, T. Kondow, T. Onishi and K. Tamaru, Surf. Sci., 59 (1976) 302.
45 C.L. Yaws, Physical Properties: A Guide to the Physical, Thermodynamic and Transport Property Data of Industrially Important Chemical Compounds, McGraw-Hill, New York, 1977.
46 G.A. Sharpataya, G.P. Panasyuk, G.P. Budova, Z.P. Ozerova, I.L. Voroshilov and V.B. Lazarev, Thermochim. Acta, 93 (1985) 271.
47 R.H. Perry and C.H. Chilton, Chemical Engineers' Handbook, 5th Edn., McGraw-Hill, Tokyo, 1973.